Submitted to *The Astrophysical Journal Letters*
Preprint typeset using LaTeX style emulateapj v. 12/14/05

arXiv:0707.0305v1 [astro-ph] 2 Jul 2007

# THE QUASAR ACCRETION DISK SIZE – BLACK HOLE MASS RELATION*

Christopher W. Morgan[1]
Department of Physics, United States Naval Academy, 572C Holloway Road, Annapolis, MD 21402; cmorgan@usna.edu

C.S. Kochanek and Nicholas D. Morgan
Department of Astronomy, The Ohio State University, 140 West 18th Avenue, Columbus, OH 43210 -1173;
ckochanek@astronomy.ohio-state.edu, nmorgan@astronomy.ohio-state.edu

and

Emilio E. Falco
Harvard-Smithsonian Center for Astrophysics, 60 Garden Street, Cambridge, MA, 02138; efalco@cfa.harvard.edu

*Submitted to The Astrophysical Journal Letters*

## ABSTRACT

We use the microlensing variability observed for nine gravitationally lensed quasars to show that the accretion disk size at 2500Å is related to the black hole mass by $\log(R_{2500}/\mathrm{cm}) = (15.6 \pm 0.2) + (0.54 \pm 0.28) \log(M_{BH}/10^9 \mathrm{M}_\odot)$. This scaling is consistent with the expectation from thin disk theory ($R \propto M_{BH}^{2/3}$), but it implies that black holes radiate with relatively low efficiency, $\log(\eta) = -1.29 \pm 0.44 + \log(L/L_E)$ where $\eta = L/(\dot{M}c^2)$. These sizes are also larger, by a factor of $\sim 3$, than the size needed to produce the observed $0.8\,\mu$m quasar flux by thermal radiation from a thin disk with the same $T \propto R^{-3/4}$ temperature profile. More sophisticated disk models are clearly required, particularly as our continuing observations improve the precision of the measurements and yield estimates of the scaling with wavelength and accretion rate.

*Subject headings:* accretion, accretion disks — dark matter — gravitational lensing — quasars: general

## 1. INTRODUCTION

Despite nearly 40 years of work on accretion disk physics, the simple Shakura & Sunyaev (1973) thin disk model and its relativistic cousins (e.g. Page & Thorne 1974; Hubeny & Hubeny 1997; Li et al. 2005) remain the standard model despite many theoretical alternatives (e.g. Narayan, Barret & McClintock 1997; De Villiers, Hawley & Krolik 2003; Blaes 2007) and some observational reservations (see Collin et al. 2002). Quasar accretion disks cannot be spatially resolved with ordinary telescopes, so we have been forced to test accretion physics through time variability (e.g. Vanden Berk et al. 2004; Sergeev et al. 2005; Cackett, Horne & Winkler 2007) and spectral modeling (e.g. Sun & Malkan 1989; Bonning et al. 2007). One notable success is the use of reverberation mapping (Peterson et al. 2004) of quasar broad line emission to calibrate the relation between emission line widths and black hole masses.

Gravitational telescopes do, however, provide the necessary resolution to study the structure of the quasar continuum source. Each gravitationally lensed quasar image is observed through a magnifying screen created by the stars in the lens galaxy. Sources that are smaller than the Einstein radius of the stars, typically $\sim 10^{16}$ cm, show time variable fluxes whose amplitude is determined by the source size (see the review by Wambsganss 2006). Smaller sources have larger variability amplitudes than larger sources. In this investigation, we exploit the optical microlensing variability in nine gravitationally lensed quasar systems to measure the size of their accretion disks, and we find that disk sizes are strongly correlated with the masses of their central black holes.

In §2 we describe the monitoring data, the lens models we use based on Hubble Space Telescope (HST) images of each system and our microlensing analysis method. In §3 we describe our accretion disk model and our results for the relationship between disk size and black hole mass. In §4, we discuss the results and their implications for thin accretion disk theory. All calculations in this paper assume a flat ΛCDM cosmology with $h = 0.7$, $\Omega_M = 0.3$ and $\Omega_\Lambda = 0.7$.

## 2. DATA AND ANALYSIS

We monitored the gravitationally lensed quasars HE 0435–1223, SDSS 0924+0219, FBQ 0951+2635, HE 1104–1805, PG 1115+080, RXJ 1131–1231, SDSS 1138+0314, SBS 1520+530 and Q 2237+030 in the $R$- and $V$-bands on the SMARTS 1.3m using the ANDICAM optical/infrared camera (DePoy et al. 2003)[2], the Wisconsin-Yale-Indiana (WIYN) observatory

---

*Based on observations obtained with the Small and Moderate Aperture Research Telescope System (SMARTS) 1.3m, which is operated by the SMARTS Consortium, the Apache Point Observatory 3.5m telescope, which is owned and operated by the Astrophysical Research Consortium, the WIYN Observatory which is owned and operated by the University of Wisconsin, Indiana University, Yale University and the National Optical Astronomy Observatories (NOAO), the 6.5m Magellan Baade telescope, which is a collaboration between the observatories of the Carnegie Institution of Washington (OCIW), University of Arizona, Harvard University, University of Michigan, and Massachusetts Institute of Technology, and observations made with the NASA/ESA Hubble Space Telescope for program HST-GO-9744 of the Space Telescope Science Institute, which is operated by the Association of Universities for Research in Astronomy, Inc., under NASA contract NAS 5-26555.

[1] Department of Astronomy, The Ohio State University

[2] http://www.astronomy.ohio-state.edu/ANDICAM/

TABLE 1
Derived Quantities

| Object | $M_{BH}$ ($10^9$ $M_\odot$) | log($R_S$/cm) (microlensing) | $\lambda_{rest}$ ($\mu$m) | $I_{corr}$ (mag) | log($R_S$/cm) (thin disk flux) |
|---|---|---|---|---|---|
| HE0435-1223 | 0.50 | $15.6^{+0.5}_{-0.7}$ | 0.260 | $20.76 \pm 0.25$ | $14.9 \pm 0.1$ |
| SDSS0924+0219 | 0.11 | $14.8^{+0.3}_{-0.4}$ | 0.277 | $21.24 \pm 0.25$ | $14.8 \pm 0.1$ |
| FBQ0951+2635 | 0.89 | $15.9^{+0.4}_{-0.4}$ | 0.313 | $17.16 \pm 0.11$ | $15.6 \pm 0.1$ |
| HE1104-1805 | 2.37 | $15.7^{+0.2}_{-0.3}$ | 0.211 | $18.17 \pm 0.31$ | $15.4 \pm 0.1$ |
| PG1115+080 | 0.92 | $16.5^{+0.5}_{-0.9}$ | 0.257 | $19.52 \pm 0.27$ | $15.1 \pm 0.1$ |
| RXJ1131-1231 | 0.06 | $15.4^{+0.3}_{-0.2}$ | 0.422 | $20.73 \pm 0.11$ | $14.8 \pm 0.1$ |
| SDSS1138+0314 | 0.04 | $14.8^{+0.6}_{-0.6}$ | 0.203 | $21.97 \pm 0.19$ | $14.6 \pm 0.1$ |
| SBS1520+530 | 0.88 | $15.5^{+0.2}_{-0.2}$ | 0.245 | $18.92 \pm 0.13$ | $15.3 \pm 0.1$ |
| Q2237+030 | 1.3 | $15.5^{+0.3}_{-0.3}$ | 0.208 | $18.03 \pm 0.44$ | $15.5 \pm 0.2$ |

Note. — $R_S$ from microlensing is the accretion disk size at $\lambda_{rest}$, the rest-frame wavelength corresponding to the center of the monitoring filter used for that quasar's lightcurve. $I_{corr}$ is the corrected (unmagnified) $I$-band magnitude. Typical $I$-band measurement errors are $\lesssim 0.1$ mag, but the larger errors on $I_{corr}$ come from uncertainties in the lens magnification. $R_S$ calculated using corrected $I$-band magnitude and thin disk theory is also unscaled; it is the disk size at the rest-frame wavelength corresponding to the center of the *HST* $I$-band filter (F814W). Both disk sizes assume an average inclination angle $i = 60°$.

using the WIYN Tip–Tilt Module (WTTM) [3], the 2.4m telescope at the MDM Observatory using the MDM Eight-K [4], Echelle and RETROCAM [5] (Morgan et al. 2005) imagers and the 6.5m Magellan Baade telescope using IMACS (Bigelow et al. 1999). We supplemented our monitoring data with published quasar light curves from Paraficz et al. (2006), Schechter et al. (1997), Wyrzykowski et al. (2003), Ofek & Maoz (2003) and Gaynullina et al. (2005). We measured the flux of each image by comparison to the flux from reference stars in the field of each frame. Our analysis of the monitoring data is described in detail by Kochanek et al. (2006).

All nine lenses have been observed in the $V$- (F555W), $I$- (F814W) and $H$-bands (F160W) using the WFPC2, ACS/WFC and NICMOS instruments on *HST*. We fit these images as combinations of point sources for the quasars and (generally) de Vaucouleurs models for the lenses as described in (Lehár et al. 2000). These provided the astrometry used for lens models and defined a constant mass-to-light ($M/L$) ratio model for the mass distribution in the lens models. We modeled each system using the *GRAVLENS* software package (Keeton 2001) to generate a series of ten models for each lens starting from a constant $M/L$ model and then adding an NFW (Navarro, Frenk & White 1996) halo. The sequence is parametrized by $f_{M/L}$, the mass fraction represented by the visible lens galaxy relative to a constant $M/L$ model. We start with the constant $M/L$ model, $f_{M/L} = 1$, and then reduce its mass in increments of $\Delta f_{M/L} = 0.1$ with the NFW halo's mass rising to compensate.

These lens models then provide the convergence $\kappa$, shear $\gamma$ and stellar surface density $\kappa_*$ needed to define the microlensing magnification patterns. We assume a lens galaxy stellar mass function $dN(M)/dM \propto M^{-1.3}$ with a dynamic range of a factor of 50 that approximates the Galactic disk mass function of Gould (2000). For the typical lens we generated 4 magnification patterns for each image in each of the 10 lens models. We gave the magnification patterns an outer scale of $20\langle R_E \rangle$, where $\langle R_E \rangle$ is the Einstein radius for the mean stellar mass $\langle M \rangle$. This outer dimension is large enough to fairly sample the magnification pattern while the pixel scale is small enough to resolve the accretion disk. We determined the properties of the accretion disk by modeling the observed light curves using the Bayesian Monte Carlo method of Kochanek (2004) (also see Kochanek et al. 2007). For a given disk model we randomly generate light curves, fit them to the observations and then use Bayesian methods to compute probability distributions for the disk size averaged over the lens models, the likely velocities of the observer, lens, source, stars, and mass. We use a prior on the mean microlens mass of $0.1 M_\odot < \langle M \rangle < 1.0 M_\odot$, but the disk size estimates are relatively insensitive to this assumption (see Kochanek 2004).

We use black hole mass estimates for the quasars that are based on observed quasar emission line widths and the locally calibrated virial relations for black hole masses (Onken et al. 2004; Greene & Ho 2007). For most systems we simply adopted the black hole mass estimates from Peng et al. (2006) based on the C IV ($\lambda$1549Å), Mg II ($\lambda$2798Å) and H$\beta$ ($\lambda$4861Å) mass-linewidth relations. For SDSS 1138+0314, we measured the width of the C IV (1549Å) line in optical spectra from the Sloan Digital Sky Survey (Adelman-McCarthy et al. 2006) and estimated the black hole mass using the normalizations of Vestergaard & Peterson (2006). These mass estimates are reliable to approximately 0.3 dex (see McLure & Jarvis 2002; Kollmeier et al. 2006; Vestergaard & Peterson 2006; Peng et al. 2006).

## 3. RESULTS

We model the surface brightness profile of the accretion disk as a power law temperature profile, $T \propto R^{-3/4}$, matching the outer regions of a Shakura & Sunyaev (1973) thin disk model. We neglect the central depression of the temperature due to the inner edge of the disk and corrections from general relativity to avoid extra parameters. The effect of this simplification on our size

---

[3] http://www.wiyn.org/wttm/WTTM_manual.html

[4] http://www.astro.columbia.edu/ arlin/MDM8K/

[5] http://www.astronomy.ohio-state.edu/MDM/RETROCAM

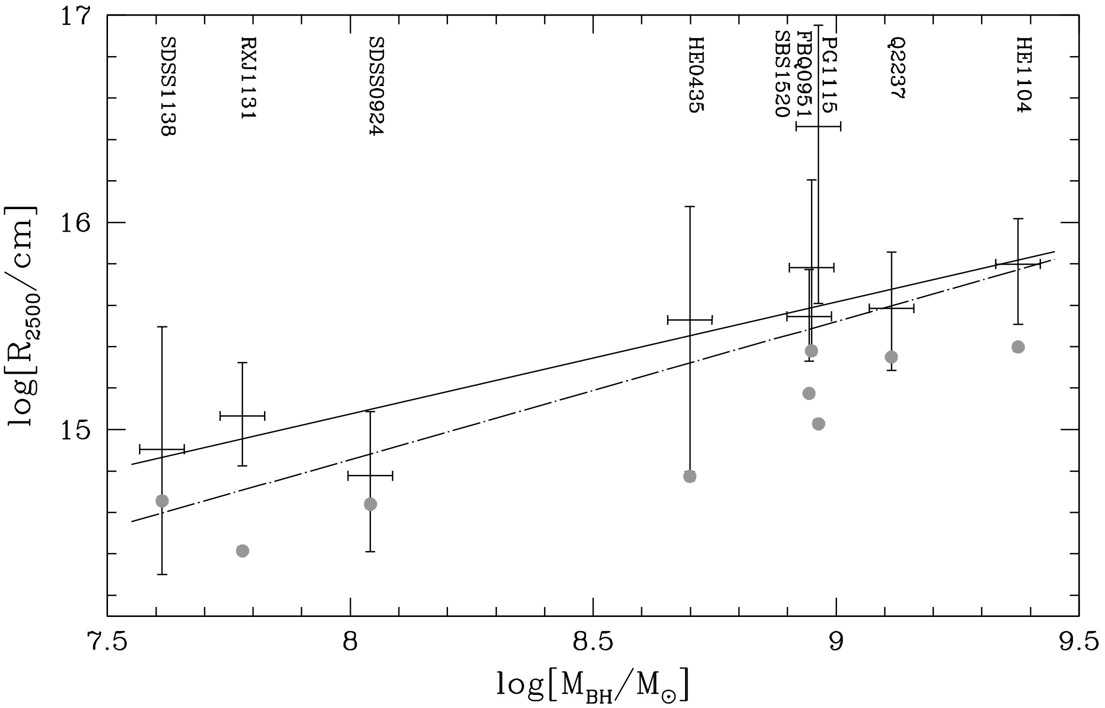

FIG. 1.— Inclination-corrected accretion disk size $R_{2500}$ versus black hole mass $M_{BH}$. The solid line shows our best power-law fit to the data and the dot-dashed line shows the prediction from thin disk theory ($L/L_E = 1$ and $\eta = 0.1$). Disk sizes are corrected to a rest wavelength of $\lambda_{rest} = 2500$Å and the black hole masses were estimated using emission line widths. The filled points without error bars are $R_{2500}$ estimates based on the observed, magnification-corrected $I$-band fluxes. They have typical uncertainties of 0.1-0.2 dex.

estimates is small compared to our measurement uncertainties provided the disk size we obtain is several times larger than the radius of the inner disk edge. We assume that the disk radiates as a black body, so the surface brightness at rest wavelength $\lambda_{rest}$ is

$$f_\nu = \frac{2h_pc}{\lambda_{rest}^3}\left[\exp\left(\frac{R}{R_{\lambda_{rest}}}\right)^{3/4} - 1\right]^{-1} \qquad (1)$$

where the scale length

$$\begin{aligned} R_{\lambda_{rest}} &= \left[\frac{45G\lambda_{rest}^4 M_{BH}\dot{M}}{16\pi^6 h_p c^2}\right]^{1/3} \\ &= 9.7\times10^{15}\left(\frac{\lambda_{rest}}{\mu\mathrm{m}}\right)^{4/3} \\ &\times\left(\frac{M_{BH}}{10^9\mathrm{M}_\odot}\right)^{2/3}\left(\frac{L}{\eta L_E}\right)^{1/3}\mathrm{cm} \qquad (2)\end{aligned}$$

is the radius at which the disk temperature matches the wavelength, $kT_{\lambda_{rest}} = h_pc/\lambda_{rest}$, $h_p$ is the Planck constant, $k$ is the Boltzmann constant, $M_{BH}$ is the black hole mass, $\dot{M}$ is the mass accretion rate, $L/L_E$ is the luminosity in units of the Eddington luminosity, and $\eta = L/(\dot{M}c^2)$ is the accretion efficiency. We can also compute the size under the same model assumptions based on the magnification-corrected $I$-band quasar fluxes measured in HST observations as

$$\begin{aligned} R_I &= 2.83\times10^{15}\frac{1}{\sqrt{\cos i}}\left(\frac{D_{OS}}{r_H}\right) \\ &\times\left(\frac{\lambda_{I,obs}}{\mu\mathrm{m}}\right)^{3/2} 10^{-0.2(I-19)}\,h^{-1}\,\mathrm{cm} \qquad (3)\end{aligned}$$

where $D_{OS}/r_H$ is the angular diameter distance to the quasar in units of the Hubble radius, $I$ is the magnification-corrected magnitude and $i$ is the disk inclination angle.

Our results are shown in Figures 1 through 3 and summarized in Table 1. For the comparison with theory and the figures, we corrected the measured sizes to $\lambda_{rest} = 2500$Å assuming the $\lambda^{4/3}$ scaling of thin disk theory and the mean inclination $\langle\cos i\rangle = 1/2$. There are two striking facts illustrated by the figures. First, we clearly see from Fig. 1 that the microlensing sizes are well correlated with the black hole mass. A power-law fit between $R_{2500}$ and $M_{BH}$ yields:

$$\begin{aligned} \log\left(\frac{R_{2500}}{\mathrm{cm}}\right) &= (15.6\pm0.2) \\ &+ (0.54\pm0.28)\log\left(\frac{M_{BH}}{10^9\mathrm{M}_\odot}\right) \qquad (4)\end{aligned}$$

which is consistent with the predicted slope from thin disk theory ($R \propto M_{BH}^{2/3}$) and implies a typical Eddington factor of $\log(L/\eta L_E) = 1.29\pm0.44$ if we fix the slope with mass to 2/3 (see Fig. 2). Kollmeier et al. (2006) estimate that the typical quasar has $L/L_E \approx 1/3$, which would indicate a radiative efficiency of $\eta = L/(\dot{M}c^2) \simeq 0.02$. This efficiency is low compared to standard models (e.g. Gammie 1999). Second, we find that microlensing sizes are well correlated with sizes estimated from thin disk theory and from the observed flux (Figs. 1 and 3), but the three size estimates show systematic offsets in scale. Most of the offset between the microlensing disk size measurements and thin disk theory size estimates could be explained by the existing uncertainties, but the off-

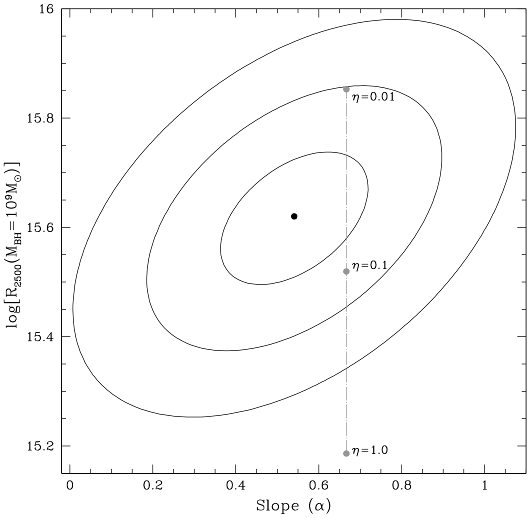

FIG. 2.— Results of the power-law fit to $R_{2500}$ as a function of black hole mass. The contours show the $1-3\sigma$ one-parameter confidence intervals for the slope $\alpha$ and the normalization $R_{2500}(M_{BH}=10^9\mathrm{M}_\odot)$ for the 2500Å accretion disk size corresponding to $M_{BH}=10^9\mathrm{M}_\odot$. The best-fit value is indicated with a black point. The filled points along the dot-dashed line are theoretical thin disk sizes for quasars radiating at the Eddington limit and with efficiencies of $\eta = L/(\dot{M}c^2) = 0.01$, 0.1 or 1.0.

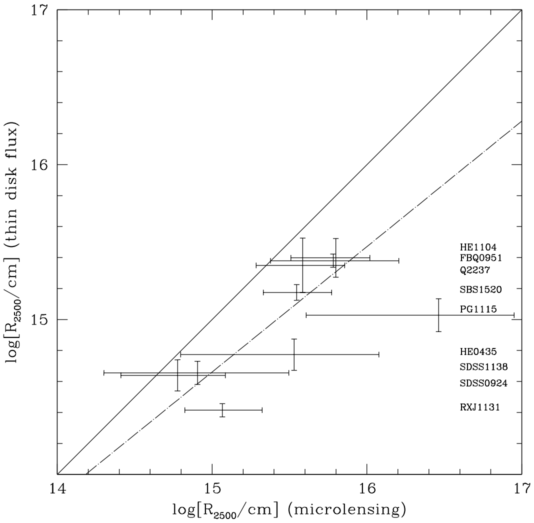

FIG. 3.— Thin disk flux size estimates versus accretion disk sizes from microlensing. For reference, the solid line indicates a one-to-one relationship between thin disk flux size estimates and microlensing measurements. The dot-dashed line is the best fit to the data. Since the data points have large errors relative to their dynamic range, the best-fit slope is consistent with unity and its average offset from the solid line is 0.4 dex.

set from the estimate based on the quasar flux is much more significant (Fig. 1). While the microlensing and flux sizes are well-correlated, the measured disk sizes are 0.4±0.3 dex larger than predicted from the observed flux. Simply put, the quasars are not sufficiently luminous to be radiating as black bodies with a $T \propto R^{-3/4}$ temperature profile. Pooley et al. (2006) also noticed this problem in their more qualitative study of lensed quasars with X-ray observations.

## 4. DISCUSSION

Are the discrepancies between our measurements and the size estimated from the disk flux due to a problem in the measurements, an oversimplification of the disk model or a fundamental problem in the thin disk model? We have tested our approach using Monte Carlo simulations of light curves and verified that we recover the input disk sizes. Our results are also only weakly sensitive to the assumed prior on the microlens masses (see Kochanek 2004, for a discussion). We will overestimate the source size if a significant fraction of the observed flux comes not from the continuum emission of the disk but from the larger and minimally microlensed line emitting regions (e.g. Sugai et al. 2007). This includes not only the obvious broad lines but also the broad Fe II and Balmer continuum emission that can represent $\sim 30\%$ of the apparent continuum flux at some wavelengths (Netzer & Willis 1983; Grandi 1982). We have experimented with adding a fraction of unmicrolensed light and found that 30% contamination does not lead to sufficiently large size changes to resolve the problem. The sizes shrink by approximately 20%. Conservatively, black hole mass estimates from the virial technique have a scatter of a factor of $\sim 3$ (McLure & Jarvis 2002; Kollmeier et al. 2006; Vestergaard & Peterson 2006; Peng et al. 2006), which contributes only 0.3 dex of scatter to the disk size estimates. The size estimates from the flux could be affected by misestimating the magnification or failing to correct for extinction in the lens galaxy, but the uncertainties in the magnifications are only a factor of $\sim 2$ at worst and none of these lenses shows significant extinction (Falco et al. 1999; Elíasdóttir et al. 2006) relative to the magnitude of the discrepancy.

The problem is also not a consequence of the obvious flaws in our simplified disk model – the neglect of the inner edge and the different temperature profile of a relativistic disk (e.g. Page & Thorne 1974). For observations at a fixed wavelength, neglecting the inner edge does not have a dramatic effect on the effective source size and the effects of relativity on the temperature profile are modest. Studies of the temperature profile in the disk with microlensing are best done by measuring the variation in source size with wavelength because size ratios can be measured much more accurately than absolute sizes. Poindexter et al. (2007) have used the wavelength dependence of the microlensing in HE 1104-1805 to derive a slope $T \propto R^{-\beta}$ or $R_\lambda \propto \lambda^{1/\beta}$ of $\beta = 0.61^{+0.21}_{-0.17}$ that is consistent with thin disk theory but would also allow a shallower temperature profile that would reduce the differences between the microlensing and flux size estimates. The next step is clearly to use more sophisticated disk models including relativity and model atmospheres such as Hubeny & Hubeny (1997) or Li et al. (2005). Mortonson et al. (2005) have argued that microlensing essentially measures the half-light radius ($R_{1/2} = 2.44R_\lambda$ for our model), so the first step should be to try to simultaneously match our size estimates and the observed fluxes assuming this to be the case, since the many additional parameters of the full disk models will make their direct inclusion in the microlensing calculations a major computational challenge.

We thank E. Agol, M. Dietrich, C. Onken, B. Peterson, M. Pinsonneault, R. Pogge and P. Osmer for discussions on quasar structure, and M. Mortonson, S. Poindexter, S. Rappaport, and P. Schechter for discussions on microlensing. This research made extensive use of a Beowulf computer cluster obtained through the Cluster Ohio program of the Ohio Supercomputer Center. Support for program HST-GO-9744 was provided by NASA through a grant from the Space Telescope Science Institute, which is operated by the Association of Universities for Research in Astronomy, Inc., under NASA contract NAS-5-26666.

*Facilities:* CTIO:2MASS (ANDICAM), Hiltner (RETROCAM), WIYN (WTTM), HST (NICMOS, ACS).

## REFERENCES

Adelman-McCarthy, J. et al. 2006, ApJS, 162, 38

Bigelow, B.C., Dressler, A.M., Schechtman, S.A. & Epps, H.W. 1999, Proc. SPIE, 3355, 12

Blaes, O. 2007 in The Central Engine of Active Galactic Nuclei, ed. L.C. Ho & J.-M. Wang (San Francisco: ASP), in press

Bonning, E.W., Cheng, L., Shields, G.A., Salviander, S. & Gebhardt, K. 2007, ApJ, 659, 211

Cackett, E.M., Horne, K. & Winkler, H. 2007, MNRAS, in press (astro-ph/07061464)

Collin, S., Boisson, C., Mouchet, M., Dumont, A.-M., Coupé, S., Porquet, D. & Rokaki, E. 2002, A&A, 388, 771

De Villiers, J.-P., Hawley, J.F. & Krolik, J.F. 2003, ApJ, 599, 1238

DePoy, D.L., Atwood, B., Belville, S.R., Brewer, D.F., Byard, P.L., Gould, A., Mason, J.A., O'Brien, T.P., Pappalardo, D.P., Pogge, R.W., Steinbrecher, D.P., & Tiega, E.J. 2003, Proc. SPIE, 4841, 827

Elíasdóttir, Á., Hjorth, J., Toft, S., Burud, I. & Paraficz, D. 2006, ApJS, 166, 443

Falco, E.E. et al. 1999, ApJ, 523, 617

Greene, J.E. & Ho, L.C. 2007, ApJ, in press

Gammie, C.F. 1999, ApJ, 522, L57

Gaynullina, E.R. et al. 2005, A&A, 440, 53

Gould, A. 2000, ApJ, 535, 928

Grandi, S.A. 1982, ApJ, 255, 25

Hubeny, I. & Hubeny, V. 1997, ApJ, 484, L37

Keeton, C.R. 2001, preprint (astro-ph/0102340)

Kochanek, C. S. 2004, ApJ, 605, 58

Kochanek, C.S., Morgan, N.D., Falco, E.E., McLeod, B.A., Winn, J.N., Dembicky, J & Ketzeback, B. 2006, ApJ, 640, 47

Kochanek, C.S., Dai, X., Morgan. C.W., Morgan, N.D., Poindexter, S.A., Chartas, G. 2007, in Statistical Challenges in Astronomy IV, ed. G.J. Babu & E.D. Feigelson, (San Francisco:ASP), in press

Kollmeier, J.A. et al. 2006, ApJ, 648, 128

Lehár, J., Falco, E.E, Kochanek, C.S., McLeod, B.A., Impey, C.D., Rix, H.-W., Keeton, C.R. & Peng, C.Y. 2000, ApJ, 536, 584

Li, L.-X., Zimmerman, E.R., Narayan, R. & McClintock, J.E. 2005, ApJS, 157, 335

McLure, R.J. & Jarvis, M.J. 2002, MNRAS, 337, 109

Morgan, C.W., Byard, P.L., DePoy, D.L., Derwent, M., Kochanek, C.S., Marshall, J.L., O'Brien, T.P. & Pogge, R.P. 2005, AJ, 129, 2504

Mortonson, M.J., Schechter, P.L. & Wambsganss, J. 2005, ApJ, 628, 594

Narayan, R., Barret, D. & McClintock, J.E. 1997, ApJ, 482, 448

Netzer, H & Wills, B. 1983, ApJ, 275, 445

Navarro, J.F. Frenk, C.S. & White S.D.M. 1996, ApJ, 462, 563

Ofek, E.O. & Maoz, D. 2003 ApJ, 594, 1104

Onken, C.A. et al. 2004, ApJ, 615, 645

Page, D.N. & Thorne, K.S. 1974, ApJ, 191, 499

Paraficz D., Hjorth J., Burud I., Jakobsson P., Elíasdóttir Á. 2006, A&A, 455, L1

Peng, C.Y., Impey, C.D., Rix, H.-W., Kochanek, C.S., Keeton, C.S., Falco, E.E., Lehár, J. & McLeod, B.A. 2006, ApJ, 649, 616

Peterson, B.M. et al. 2004, ApJ, 613, 682

Pooley, D., Blackburne, J.A., Rappaport, S., Schechter, P.L. & Fong, W.-F. 2006 ApJ, 648, 67

Poindexter, S.A., Morgan, N.D., Kochanek, C.S. & Falco, E.E. 2007, in preparation

Schechter, P.L. et al. 1997, ApJ, 475, L85

Sergeev, S.G., Doroshenko, V.T., Golubinskiy, Y.V., Merkulova, N.I. & Sergeeva, E.A. 2005, ApJ, 622, 129

Shakura, N.I. & Sunyaev, R.A. 1973, A&A, 24, 337

Sugai, H. et al. 2007, ApJ, 660, 1016

Sun, W.-H. & Malkan, M.A. 1989, ApJ, 346, 68

Vanden Berk, D.E. et al. 2004, ApJ, 601, 692

Vestergaard, M. & Peterson, B.M. 2002, ApJ, 641, 689

Wambsganss, J. 2006, in Saas-Fee Advanced Course 33, Gravitational Lensing: Strong, Weak and Micro, ed. G. Meylan, P. Jetzer. & P. North, (Berlin:Springer), 453

Wyrzykowski, L. et al. 2003, Acta Astron., 53, 229